Preprints.org

Communication

Polyclonal Aptamers in Fluorescence-Based Assays for Rikenella microfusus-Specific Gut Microbiome Analyses

Yiting Zhang , Hu Xing , Grigory Bolotnikov , Markus Kraemer , Nina Gotzmann , Uwe Knippschild , Ann-Kathrin Kissmann , Frank Rosenau *

Communication

Polyclonal Aptamers in Fluorescence-Based Assays for _Rikenella microfusus_-Specific Gut Microbiome Analyses

Yiting Zhang [1,†], Hu Xing [1,†], Grigory Bolotnikov [1], Markus Krämer [1], Nina Gotzmann [1], Uwe Knippschild [2], Ann-Kathrin Kissmann [1,3,‡] and Frank Rosenau [1,*,‡]

[1] Institute of Pharmaceutical Biotechnology, Ulm University, Albert-Einstein-Allee 11, 89081 Ulm, Germany

[2] Department of General and Visceral Surgery, Surgery Center, Ulm University, Albert-Einstein-Allee 23, 89081 Ulm, Germany

[3] Max-Planck-Institute for Polymer Research Mainz, Ackermannweg 10, 55128 Mainz, Germany

[*] Correspondence: frank.rosenau@uni-ulm.de

[†] These authors contributed equally to this work.

[‡] These authors contributed equally to this work.

Abstract: _Rikenella microfusus_ is an essential intestinal probiotic with great potential. The latest research shows that its imbalance in the intestinal flora is related to the occurrence of various diseases, such as intestinal diseases, immune diseases, and metabolic diseases. _Rikenella_ may be a target or biomarker for some diseases, providing a new possibility for preventing and treating these diseases by monitoring and changing the abundance of _Rikenella_ in the intestine. However, the current detection methods have disadvantages such as long detection time, complicated operation, and high cost, which seriously limit the possibility of clinical application of this new treatment method. Therefore, developing rapid and low-cost detection methods has become an urgent problem to be solved. In this study, we used _Rikenella_ as the target bacterium, meanwhile including five other prominent gut bacteria _Akkermansia muciniphila_, _Allobaculum stercoricanis_, _Blautia producta_, _Roseburia intestinalis_ and _Parabacteroides distasonis_ as control organisms. The aptamer library R.m-R13 was evolved with high specificity and strong affinity ($K_d = 9.597$ nM) in an iterative Cell-SELEX process after 13 rounds of selection. _R. microfusus_ can efficiently be discriminated from other major gut bacteria in complex mixtures in different analysis techniques including fluorescence microscopy or fluorometric suspension assays and even in human stool samples. These preliminary results open new avenues towards the development of aptamer-based microbiome bio-sensing applications for fast and reliable _R. microfusus_ monitoring.

Keywords: DNA aptamer; biosensor; Cell-SELEX; in vitro diagnostic; _Rikenella microfusus_

1. Introduction

More than 100 trillion microorganisms are on and in the human body, which is inextricably linked to health and disease and plays a vital role. Research on intestinal flora has developed in recent years, revealing definitive evidence of its association with digestive tract disorders and neurological, endocrine, cardiovascular, reproductive, and other diseases [1–4]. _R. microfusus_, as a significant gut bacterium, has demonstrated a close relationship with the onset of numerous disorders, which has recently become a hot research topic. It was first isolated by Kaneuchi and Mitsuoka in 1978 from many fecal or cecum specimens from calf, chicken, and Japanese quail [5]. The abundance of _Rikenella_ in the intestine of patients with inflammatory bowel disease (IBD) is significantly suppressed compared to healthy patients [6–8]. In mice with autoimmune disease, _Rikenella_ was also substantially lower than expected [9]. _Rikenella_ appears to be a crucial gut microbiome member and potential probiotic probably being essential for reducing intestinal inflammation [10,11]. Short-chain carboxylic acids, including succinic acid, propionic acid, acetic acid, and alcohols as typical

metabolites of *Rikenella*, can effectively improve the intestinal flora environment and enhance microbial abundance [6]. Evidence exists that *Rikenella* can help intestinal cells to form tight junctions, which can help epithelial cells differentiate, thereby strengthening the intestinal barrier [12,13]. As the regulation of intestinal microflora is an essential factor in the fight against diarrhea, another study further demonstrated that *Rikenella* is also one of the effective anti-diarrhoeal probiotics, with its abundance negatively correlated with the diarrhea index [14]. In the mouse allergy models, the allergic symptoms were significantly improved by reducing the abundance of *Rikenella* [15]. In another group of mouse obesity models the abundance of *Rikenella* in the intestine of these mice was significantly lower than that of lean mice [16]. Interestingly, increasing the amount of *Rikenella* in the intestine of mice even markedly decreased insulin resistance in type 2 diabetes [17–19]. Intestinal barrier dysfunction and bacterial translocation can lead to inflammation in chronic kidney disease (CKD) [20,21]. Early renal complications caused by diabetes can be prevented by modulating the intestinal flora. In one study, intestinal permeability and inflammation in mice were improved by altering the intestinal microbiota, including *Rikenella*, through pharmacological treatment [22]. In addition, *Rikenella* is significantly dysregulated in depressed patients, and receiver operating characteristic (ROC) curves show that *Rikenella* may be a potential biomarker for depression-like behavior in mice [23,24]. What is more intriguing is that, while certain microflora is diminished or missing in many diseases, they are unusually plentiful in healthy individuals, suggesting that they may serve as a target or biomarker for the therapy of various disorders. Certain retinal neurodegenerative diseases are also associated with gut microbial homeostasis; *Rikenella* is widespread in healthy gut microbiomes but is essentially absent in mouse models of retinal disease [25,26]. *Rikenella* is abundant in HIV-negative subjects but progressively declined or depleted in untreated HIV patients [27–30]. Metabolites produced by specific microbiota are also involved in several lipid metabolisms, membrane transport, and other pathways that are considered relevant to the pathogenesis of Alzheimer's disease (AD) [31]. *Rikenella* was scarce in AD mice, but this was quickly reversed after gut flora-targeted therapy, suggesting that *Rikenella* may be a potential target for the treatment of AD [32]. Gut flora can be involved in treating of AD-related cognitive impairment by controlling the dysregulation of pyrimidine metabolism, and *Rikenella* may therefore be a significant biological marker for AD [33].

Using the Cell-SELEX method, aptamer libraries can be obtained with high affinity and selectivity after repeated selection *in vitro*. Aptamers offer numerous benefits over antibodies, including low cost, low molecular weight, non-immunogenicity, and simplicity of modification. As a result, they have attracted much attention in recent years for use in drug administration, targeted therapeutic, and diagnostic applications [34]. Since its initial application in 1990, SELEX technology has evolved. Significant advances have been achieved in the design of construction and use of aptamers, such as making the screening process more efficient, less costly, and less time-consuming [35–37]. SELEX is an iterative process, in which the screening procedure includes binding of the aptamers, isolation of target bound molecules and subsequent PCR amplification. This results in culminating of sequences with target affinity and efficiently enrichment of a library of nucleic acid aptamers with increasing affinity and specificity towards the target structure (i. e. cells in whole cell SELEX) after repeated rounds of evolution with increasing selection pressure by harshening the binding/ washing conditions [38,39].

In our previous studies, we have facilitated our real-time monitoring of the screening/selection process by Cy5 fluorescent labeled DNA aptamers and direct measurement of aptamer binding to target cells by changes of fluorescence intensities on the cells. This technique we introduced as the Flucell-SELEX [40–44]. In order to boost the SELEX screening pressure and improve stringency, a mixture of five other intestinal bacteria was used in a counter-selection, including *A. muciniphila, A. stercoricanis*, *B. producta*, *R. intestinalis,* and *P. distasonis* in this study (Figure 1). The final aptamer library, R.m-R13, has a strong affinity for *R. microfusus* and enables efficient quantification of this bacterium in the mixed model intestinal flora. As far as we know, we are the first to isolate and directly use an aptamer library to identify or label this probiotic strain, providing a solid foundation

for the subsequent development and optimization of more accessible and cost-effective assays and biosensors for the clinical detection and subsequent fast and precise quantification of *Rikenella*.
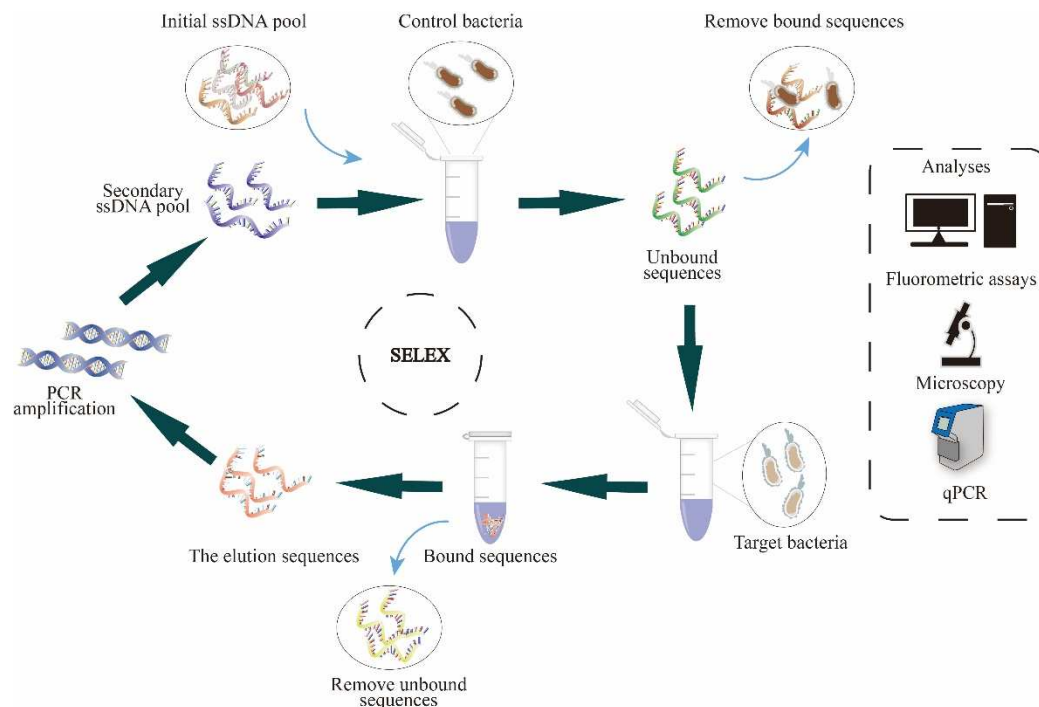
Figure 1. The screening efficiency was enhanced by incubating the initial library with a mixture of control bacteria, including *A. muciniphila*, *A. stercoricanis*, *B. producta*, *R. intestinalis*, and *P. distasonis*, during the initial rounds of selection. Counter-SELEX was used to eliminate aptamers unbound to target bacteria. Subsequently, the aptamers obtained in the previous evolution round were incubated with the target bacterium *R. microfusus* for target SELEX. After repeating several rounds of screening/selcection, we obtained aptamer eluates to obtain new pools of enriched DNA by PCR amplification. Ultimately, we analyzed the polyclonal aptamer libraries we obtained that specific binding target cells in various ways, including fluorescence analysis, fluorescence microscopy observation, and qPCR quantitative analysis.

2. Results

In 13 rounds of SELEX, we have evolved the particular DNA aptamer library R.m-R13 against the gut bacterium *R. microfusus* by using the FluCell-SELEX technique. We performed positive selection for *R. microfusus* in the first four rounds to enhance the number of specific DNA aptamers by compensating a dearth of single specific aptamers as a considerable limitation of the procedure in the initial library. From the fifth round onwards, adding a counter-selection step to the procedure using the negative control bacterial mixture prior to the positive selection resulted in a more efficient development of the specific aptamer library indicated by the onset of a positive fluorescence signal starting with the fifth SELEX cycle (fig. 2 a). Since rounds 5-8 proceeded steadily but rather slowly, the number of counter-selection bacteria to enhance the pressure from round 9 onwards. As a result, the binding intensity of the aptamer library increased drastically. In rounds 11 and 12, the fluorescence signal leveled off but was reduced by 25% after the 13th round and hence we considered the screening process as completed (Figure 2a) [45]. Using the ensemble of the five negative control gut bacteria, we then determined the specificity of the polyclonal aptamer libraries for *R. microfusus* surface targets in rounds 11–13, respectively.

The progressive increase in library specificity indicated that the ability of the aptamer library to distinguish between *R. microfusus* and the control strains was effectively improved. The aptamer library R.m-R13 obtained in the final productive round 13 showed the highest level of specificity, although the affinity was somewhat weaker than in round 12 (Figure 2b). Further, the melting curves

of the aptamer libraries originating from the SELEX rounds was analyzed in qPCR reactions. Tm indicates the average melting temperature profile and the melting temperatures S_{Tm} and E_{Tm} at the start and the end of the SELEX, were determined, respectively. During the SELEX process proceeding, the library melting temperature raised from 63°C (S_{Tm}) to 74°C (E_{Tm}) (Figure 2c). The effective increase in maximum library melting temperature originates from the enrichment of DNA aptamers with high GC content in the library, which generally tend to have better secondary structure stability and can provide more potential hydrogen bonds towards target atoms. In order to compare the degree of shift in the melting curve during the screening process, we quantified the relative ddRn/dT values for each screening round at the peak temperatures of S_{Tm} and E_{Tm} to provide a measure of the Tm shift in the screening process, where the ddRn/dT values gradually decrease at S_{Tm} and, in contrast, increased and eventually stabilized at E_{Tm} (Figure 2d).
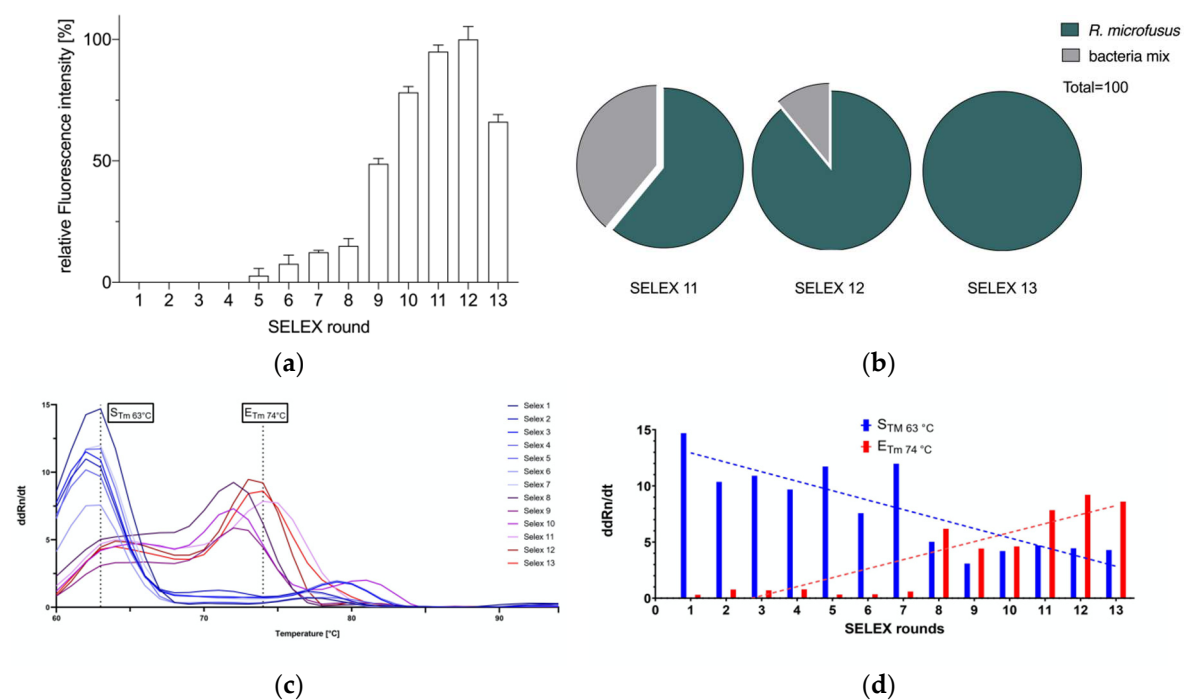
Figure 2. (a) Affinity and (b) specificity assay for *R. microfusus*; using the aptamer library R.m-R13. The specificity of the polyclonal aptamer library obtained in rounds 11-13 increased progressively compared to the mixture of the other five intestinal bacteria *B. producta*, *A. muciniphila*, *R. intestinalis*, *A. stercoricanis*, and *P. distasonis*. All experiments were performed using five pmol aptamer and 10^8 cells, and fluorescence intensity was measured at 635 nm excitation and 670 nm emission. All experiments were performed in three sessions (*N*=3); (c) Melting curves of the prominent temperature peaks, including S_{Tm} at the start and E_{Tm} at the end of SELEX; (d) peak shift analyses for S_{Tm} and E_{Tm}, linear regression fitted to ddRn/dT (fluorescence change/temperature change) with different SELEX rounds.

To quantitatively evaluate the strength of binding affinity of the aptamer library R.m-R13, we further obtained the dissociation constant (K_d) of R.m-R13 by co-incubating quantitative *R. microfusus* with different concentrations of Cy5-labelled aptamer library (Figure 3a), which was determined to have a K_d value of 9.597 nM, indicating that the selected aptamer R.m-R13 has a high affinity for *R. microfusus*. At the same optical density settings, fluorescence microscopy was used to identify the binding of the aptamer library R.m-R13 to the target bacterium *R. microfusus* and five other enteric bacteria, including *B. producta*, *A. muciniphila*, *R. intestinalis*, *A. stercoricanis*, and *P. distasonis*. The results showed that the aptamer library R.m-R13 exhibited intense labeling of *R. microfusus* while failing to label the other five control bacteria (Figure 3b). Next, we analyzed the ability of the aptamer library to retrace *R. microfusus* in different proportions of mixed bacteria, and the fluorescence intensity revealed a significant positive linear correlation with the number of target bacteria (R^2 =

0.9835), and the aptamer library was able to track an increase in *R. microfusus* numbers successfully (Figure 3c).
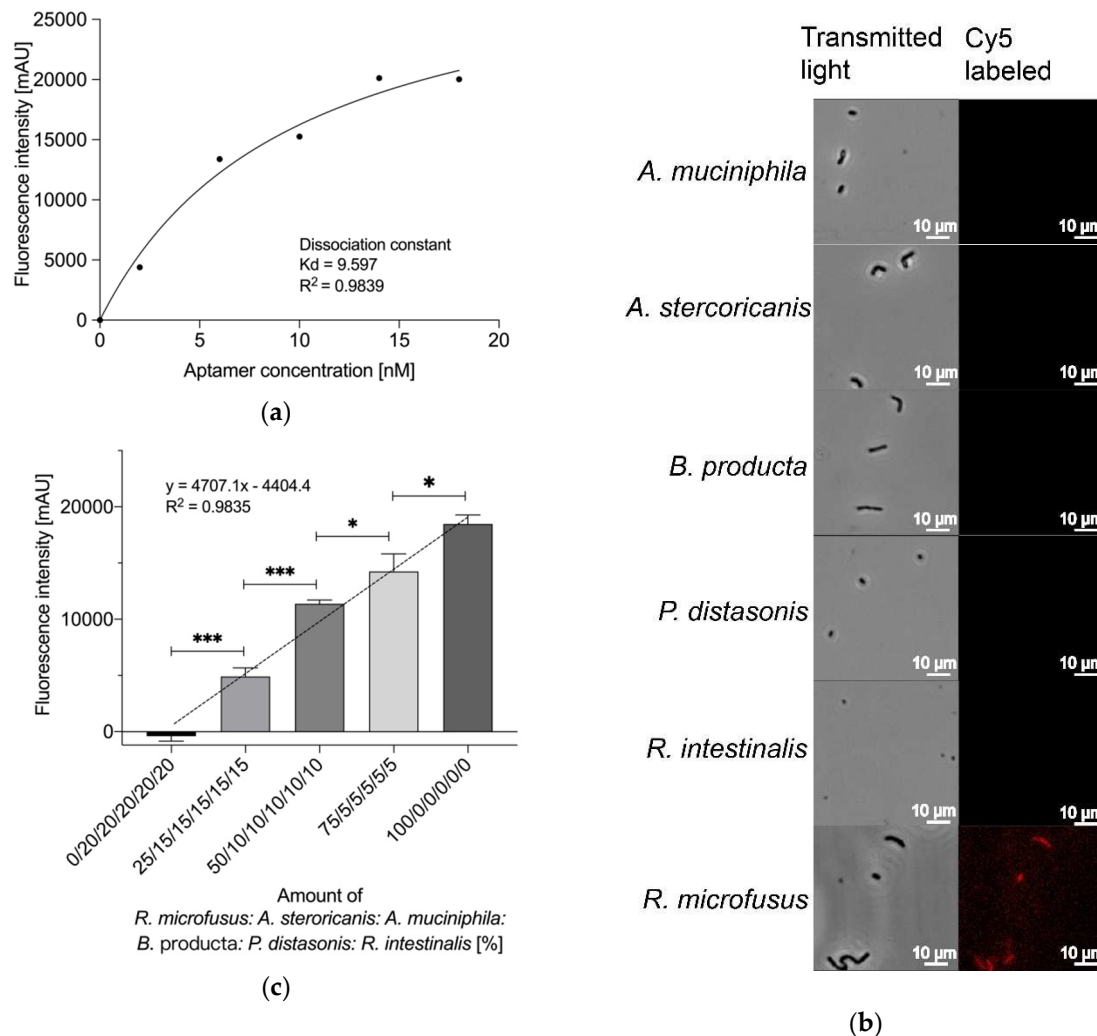

Figure 3. (a) Determination of the dissociation constant for the aptamer library R.m-R13 with a K_d of 9.597 nM and a deviation of 0.9839 in the coefficient of determination R^2; (b) Fluorescence microscopy observations of the aptamer library R.m-R13 bound to *R. microfusus*, *B. producta*, *A. muciniphila*, *R. intestinalis*, *A. stercoricanis,* and *P. distasonis*. Cy5-labeled R.m-R13 displayed a strong fluorescent signal bound to *R. microfusus*, whereas the other five bacteria as controls delivered as expected no signals. (c) Quantification of the aptamer library R.m-R13 on *R. microfusus* in a mixture that included *B. producta*, *A. muciniphila*, *R. intestinalis*, *A. stercoricanis,* and *P. distasonis*, mixed in different proportions at the same OD. All experiments were performed using five pmol aptamers in 10^8 cells, and all experiments were performed in three runs (*N*=3). *p* values < 0.05 were considered significant. *** denotes *p* < 0.001.

To further characterize the aptamer library R.m-R13 as binding entities for biosensing applications, we evaluated the detection limit of the library. Aptamers were quantified by co-incubation with various *R. microfusus* numbers to generate a standard fluorescence intensity curve as a function of bacterial count (Figure 4a).

With *R. microfusus* levels of more than 10^2 in 1 mL samples, the fluorescence intensity was positively correlated with the number of bacteria. (R^2 = 0.9889). Considering the plenty of bacteria in fecal samples, it is reasonable to assume that the aptamer library R.m-R13 could detect the abundance of *R. microfusus* from even a low amount of fecal samples. To test this hypothesis, we selected feces from two healthy volunteers (Proband 1 and Proband 2 in Figure 4b). We used the aptamer library

R.m-R13 and NGS to determine the abundance of *Rikenella* in the subject samples, respectively. First, we set the relative fluorescence intensity of the control *R. microfusus* at 100% by the assay using the aptamer library.

In contrast, the relative fluorescence intensity of the experimental group was expressed as a percentage of *Rikenella* in the Proband fecal samples, with fluorometric results of 0.3% and 1.3%, respectively. The corresponding standard deviations were individually 1.1% and 0.7%. Additionally, by NGS, we obtained 0.34% and 1.1% of *Rikenella* in fecal bacteria for Proband 1 and Proband 2, respectively (see Tables S2 and S3, Supplementary Material). As a result, we believe that the aptamer R.m-R13 can fully satisfy requirements for both the sensitivity and accuracy of *Rikenella* detection in practical applications, which also provides a robust theoretical foundation for installing the biochip in the future.
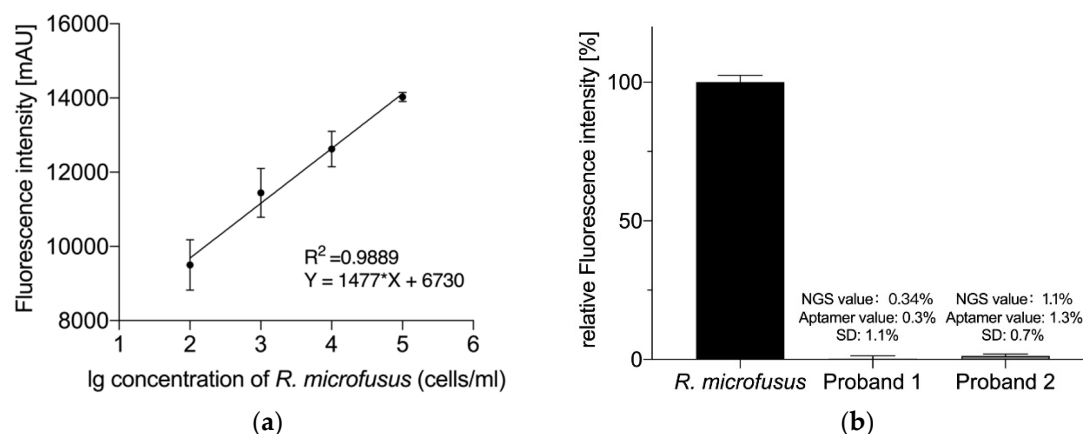
Figure 4. (a) Sensitivity assay of the aptamer library R.m-R13. In a 1 mL reaction system containing five pmol of the aptamer library, R.m-R13 showed a significant positive correlation between the number of bacteria and fluorescence intensity for *R. microfusus* numbers greater than 10^2 ($R^2 = 0.9889$), and therefore the minimum detection limit for the aptamer library was determined to be 10^2 cells/mL; (b) Comparison of *Rikenella* abundance measurements in fecal samples from the aptamer library R.m-R13 and 16s rRNA NGS (see Tables S2 and S3, Supplementary Material). "NGS values" represent the actual *Rikenella* content in fecal bacteria. The "Aptamer value" represents the amount of *Rikenella* in fecal bacteria determined using the aptamer library R.m-R13. Error bars indicate the standard deviations of the experiments conducted in triplicate.

3. Discussion

The correct abundance of *R. microfusus*, one of the most critical potential intestinal bacteria, has been associated with intestinal diseases, metabolic diseases, HIV, and AD, and therefore quantitative monitoring of the composition of intestinal flora may be crucial for the prevention and potential therapy of these diseases [11,21,30,31]. However, intestinal flora assays such as 16S rRNA gene sequencing, and bacterial group/species quantitative polymerase chain reaction (qPCR) have the considerable disadvantages of being time-consuming, complex, costly and often require specialized laboratories and personnel. Developing a rapid and easy-to-use method to monitor intestinal flora is challenging but an attractive investment into the future of medical microbiome research. Therefore, it is urgent to develop a quick and convenient way to monitor intestinal flora and its changes [46] where the use of biosensors enables rapid, simple, low-cost, and quantitative detection. Aptamers as nucleic acid ligands can be repeatedly denatured and denaturalized under heat, different salt concentrations, and metal chelators. They can be modified and solidified, are highly stable, and easily labeled with the target moiety, thus gradually replacing antibodies as binding entities in bioassays in recent years [47,48].

Living cells, exhibiting a natural 3D structure of epitopes on their cell surfaces, are targets in the whole Cell-SELEX variant used here. Compared to inactivated cells as targets, this natural conformation of surface molecules is crucial for productive aptamer screening [49]. Whole-cell

screens tend to have higher fidelity than screens using purified proteins and are therefore, more versatile [50]. The aptamer library R.m-R13, obtained after 13 rounds of cell-SELEX, allows the specific detection of *Rikenella* in complex intestinal flora mixtures and human feces. R.m-R13 exhibits a low dissociation constant (K_d = 9.597 nM), ensuring a high affinity.

Furthermore, in fluorescence assays, the aptamer library R.m-R13 clearly showed a binding preference for the target bacterium *R. microfusus* compared to controls *B. producta*, *A. muciniphila*, *R. intestinalis*, *A. stercoricanis* and *P. distasonis* demonstrating its *R. microfusus*-specific recognition potential and possible use as a diagnostic tool. Compared to the levels of *Rikenella* in human fecal samples identified by 16S rRNA next-generation sequencing (0.34% and 1.1% for Proband 1 and Proband 2, respectively), the levels of *R. microfusus* obtained by fluorescence analysis of the aptamer R.m-R13 were broadly consistent with the NGS assay results (0.3% and 1.3%). However, NGS needs a method for obtaining valid, complete, and reliable bacteria numbers categorized below the genus [44,51]. Therefore, we could not determine actual *R. microfusus* content from the NGS assay results alone. As we did not evaluate the specificity of the aptamer library R.m-R13 for another subgenus of *Rikenella*, we suggest that aptamer binding occurs at the level below the genus, and we, therefore, consider that the results of the aptamer library assay correspond to the levels of all bacteria of the genus *Rikenella* in fecal samples.

We currently aim on developing electronic biosensors for quantifying and differentiating gut bacteria as biomarkers involving polyclonal aptamer libraries as binding entities on graphene FET sensors [52]. *Rikenella* can serve as a potential target and biomarker for a set of diseases and constant monitoring of its abundance may help to develop not only a better understanding of dysbiosis in health and disease development, but may also facilitate dedicated probiotic treatments of bacterial imbalances as reasons for disease. The successful development of the aptamer library R.m-R13, which explicitly can label *Rikenella*, represents the first and most important milestone of our way to a specific *R. microfusus* aptasensor, thereby paving new avenues for new microbiome monitoring techniques as a promising amendment to the portfolio of diagnostic tools in the near future.

4. Materials and Methods

4.1. Cell Lines and Cell Culture

The bacteria strains *R. intestinalis* (DSM-14610), *P. distasonis* (DSM-29491), *A. muciniphila* mucT (DSM-22959), *A. stercoricanis* (DSM-13633), *B. producta* (DSM-29491), and *R. microfusus*, (DSM-15922) were cultivated in Schaedler-Bouillon Medium (Carl Roth GmbH + Co. KG, Karlsruhe, Germany) at 37∘C under anaerobic conditions.

4.2. Cell Lines and Cell Culture

A random sequence library (TriLink BioTechnologies, Inc, San Diego, CA, USA) was synthesized and purified. The sequence was as follows: 5'-TAGGGAAGAGAGAGAGGACATATGAT-$N_{(40)}$-TTTGACTAGTACATGACCACTTGA-3'. The initial library consists of three parts: a random sequence of 40 nucleotides in the middle and a fixed sequence of 23 nucleotides at each end that can be precisely and complementarily paired with primers, including Cyanine 5-labeled forward primers 5'-Cy5-TAGGGAAGAAGGAGAGAGATGATA-3' and phosphate-labeled reverse primers 5'-phosphate-TCAGTGTCATGTACTAGTCAA-3' (Biomers.net GmbH, Ulm, Germany).

4.3. Cell-SELEX

Cell SELEX includes counter SELEX as well as target SELEX. Counter SELEX uses bacteria mix including *B. producta*, *A. muciniphila*, *R. intestinalis*, *A. stercoricanis,* and *P. distasonis* to obtain aptamers that do not bind to bacteria combination, which can be further incubated with *R. microfusus* by target SELEX to acquire a library of aptamers that specifically bind to *R. microfusus*. Cell SELEX can be divided into the following steps.

4.3.1. Cell Pretreatment

Six bacteria were incubated under anaerobic conditions for 10-15 hours, centrifuged at 9000 xg for 1 min, and the OD_{600} of the bacterial solution was adjusted to 1 after washing once with 1×DPBS buffer.

4.3.2. Aptamer Library Activation

0.5 nmol of the initial library or 10/5 pmol of the ssDNA library was added to 500 μL of 1×DPBS and incubated at 95°C for 5 min, followed by an ice bath for 5 min. The final incubation was at room temperature for 20 min to ensure that the aptamers had the same 3D structure.

4.3.3. Screening

The activated library was incubated with the control five cells mixture for 1 h at 37°C and centrifuged at 3000 xg for 2 min. The supernatant was pipetted into a new 1.5 mL centrifuge tube, BSA (100 mg/mL) and tRNA (10 mg/mL) were added, gradually increasing as the screen progressed to improve stringency, and subsequently incubated with *R. microfusus* for 30 min at 37°C. The supernatant was removed by centrifugation at 3000 xg for 2 min and the pellet was washed with 1×DPBS to discard unbound nucleic acids (see Table S1, Supplementary Material).

4.3.4. Elution

The washed bacteria pellet was resuspended in 100 μL of 1×DPBS and incubated for 5 min at 95°C to disrupt the aptamer 3D structure and separate it from the cells. The supernatant was then collected by centrifugation at 11,000 xg for 1 min.

4.3.5. Acquisition of Secondary Libraries

SELEX collected aptamers by PCR amplification in a total reaction volume of 50 μL: 10 μL 5× Herculase II reaction buffer, 1.25 μL dNTPs 10 mM, 0.125 μL Cy5-Primer (biomers.net GmbH, Ulm, Germany) 10 μM, 0.125 μL phosphate-Primer (biomers.net GmbH, Ulm, Germany) 10 μM, 0.25 μL Herculase II Fusion DNA Polymerase (Agilent Technologies, Inc., Santa Clara, CA, USA), 1 μL template DNA and water.

The amplification conditions were as follows: 2 min at 95 °C; followed by 25 cycles of 95 °C for 30 sec; 56 °C for 30 sec, 72 °C for 10 sec, and a final extension of 72 °C for 2 min. The obtained PCR products were purified using an optimized purification kit (MACHEREY-NAGEL GmbH & Co. KG, Düren, Germany). The obtained PCR products were purified by using an optimized purification kit (MACHEREY-NAGEL GmbH & Co. KG, Düren, Germany), catalyzed by λ-exonuclease to single-stranded DNA (New England Biolabs, Ipswich, MA, USA), and the treated samples were purified by an optimized PCR purification kit (MACHEREY-NAGEL GmbH & Co. KG, Düren, Germany) to obtain new DNA pools for subsequent SELEX. To get greater yields from the PCR products and subsequent ssDNA purification, 1.5 times more isopropanol and 10 μL of NaAc solution (pH = 5) had to be added to the necessary buffer.

4.3.6. Binding Assay

After pretreatment with *R. microfusus* (see section 4.3.1), *R. microfusus* (1 mL OD_{600}=0.1) was mixed with 5 pmol of Cy5-labelled activated aptamer library in 500 μL of 1×DPBS and incubated at

37°C for 30 minutes. The supernatant was removed after centrifugation at 3000 xg for 2 min, washed once, and the pellet was resuspended with 100 μL of 1×DPBS buffer to obtain the eluted aptamers combined with cells. Finally, fluorescence intensity was measured using an Infinite M200 spectrophotometer (TECAN Trading AG, Männedorf, Switzerland) at 635 nm excitation and 670 nm emission.

4.4. Determination of High Specificity Aptamer Libraries

4.4.1. Semi-Quantitative Analysis of R. microfusus

After pretreatment of all bacterial solutions (see Section 4.3.1), *R. microfusus* and control strains (including five other enteric bacteria *B. producta*, *A. muciniphila*, *R. intestinalis*, *A. stercoricanis,* and *P. distasonis*) were mixed at different ratios. *R. microfusus* was gradually reduced from 100% to 0%. The 5 pmol activated Cy5-labelled aptamer library was then co-incubated with the bacteria in 500 μL of 1×DPBS system for 30 minutes at 37°C. After post-treatment, a comparison of the change in fluorescence intensity across the groups concerning *R. microfusus* content was made (see section 4.3).

4.4.2. Affinity Analysis

R. microfusus was pretreated (see section 4.3.1). Aptamer library affinity ligation assays were performed by co-incubating different concentrations of aptamer libraries with equal amounts of *R. microfusus* (1 mL OD_{600} = 0.1) in 500 μL of 1×DPBS at 37°C for 30 min. Finally, the aptamer concentration was fitted to the corresponding bound fluorescence intensity by using GraphPad PRISM 8 (GraphPad Software, San Diego, CA, USA) to determine the dissociation constant (K_d) of the fluorescent aptamer by calculating the equation $Y = B_{max} \times X/(K_d + X)$, where Y = measured fluorescence, Bmax = maximum fluorescence and X = concentration of the aptamer.

4.4.3. Fluorescence Microscopy

Bacterial solutions of six bacteria, *R. microfusus, B. producta, A. muciniphila, R. intestinalis, A. stercoricanis*, and *P. distasonis*, were pretreated by above method (see section 4.3.1). 5 pmol of activated aptamer library in 500 μL 1×DPBS was incubated separately with each bacterium (1 mL OD_{600}=0.1) for 30 min at 37°C. After centrifugation at 3000 xg for 2 min, the supernatant was removed. The pellet was washed once with 500 μL of 1×DPBS and then resuspended with 500 μL of 1×DPBS. 10 μL of each bacterial mixture was then added to slides, and fluorescence imaging of each group was obtained using a fluorescence microscope, using a Leica DMi8 code (Leica Microsystems CMS GmbH, Wetzlar, Germany) at ×40 magnitude (excitation: 590-650 nm, emission: 662-738 nm) under transmitted light from a Y5 filter.

4.4.4. Real-Time PCR

Eluates from SELEX rounds 1 to 13 were collected separately, and the aptamers obtained from each screening round were quantified. Samples were stained with SYBR Green I (final concentration 0.5×) (Sigma-Aldrich, St. Louis, MO, USA) and quantified in real-time by qTOWER³G touch (Analytik Jena GmbH, Jena, Germany) under the following thermal cycling conditions: an initial step of 3 min at 94 °C, followed by 40 cycles of 30 sec at 94 °C, 30 sec at 56 °C, and 10 sec at 72 °C. A master mix was prepared for each reaction batch   using Herculase II Fusion DNA Polymerase (Agilent Technologies, Inc., Santa Clara, CA, USA) and 100 mM unmodified primers (forward primer: 5′-TAG GGA AGA GAA GGA CAT ATG AT-3′; reverse primer: 5′- TCA AGT GGT CAT GTA CTA GTC AA-3′) (biomers.net GmbH, Ulm, Germany) This was followed by a melting curve analysis consisting of 40 melting cycles starting at 60°C to a temperature of 95°C. Linear regression analysis was performed to test the relationship between ddRn/dT (change in fluorescence divided by change in temperature) and the different SELEX rounds. and the Ct value were determined.

4.5. Analysis of R. microfusus Abundance in Human Stool Samples

4.5.1. Human Stool Samples

In this investigation, two healthy volunteer stool samples were utilized. Volunteers were recruited from Ulm University and signed a written informed consent form. Permission was obtained from the local ethics committee of the University of Ulm (No. 30/20). In addition, the study was designed and conducted following the regulations for using human research participants and in strict accordance with the standards set by the Declaration of Helsinki.

4.5.2. Stool Bacteria Extraction

The fecal samples were weighed and vortexed in 1×DPBS buffer for 1 minute until no fecal particles were visible. The undissolved fecal pellets, as well as food residues, were then removed by filtration. The filtrate was centrifuged at 9000 xg for 1 min, washed three times with 1×DPBS buffer, and finally adjusted to a bacterial concentration of OD_{600} of 1.

4.5.3. Analysis Based on NGS

Fecal samples were collected by using INTEST.Pro (Biomes Laboratory, Wildau, Germany), which were subsequently measured and analyzed by Biomes Laboratory (Wildau, Germany) to detect fecal bacterial abundance using 16s rDNA NGS according to Lilja *et al.*, 2021 [53].

4.5.4. Analysis Based on the Aptamer Library R.m-R13

The *R. microfusus* (see Section 4.3.1) and fecal samples (see Section 4.5.2) were pretreated. *R. microfusus* (10^8 CFU) and fecal bacteria (10^8 CFU) were then incubated separately with 500 μL of 1×DPBS (containing 5 pmol of activated aptamer library) for 30 min at 37°C (see section 4.3.2), and the fluorescence intensity was measured after elution.

5. Conclusions

In summary, we have developed the first DNA aptamer library with excellent selectivity and good binding affinity for the probiotic *R. microfusus*. The aptamer library selected after 13 rounds of screening characterized the binding of the target with a K_d value of 9.597 nM. It influenced the detection and measuring of *R. microfusus* from a mixture of bacteria. Even in human fecal samples, it still exhibits excellent discrimination. The aptamer library's detection capability is similar to the results of NGS data, which might be used to create a biosensor with rapid detection and lower cost.

References

1. Strandwitz, P. Neurotransmitter modulation by the gut microbiota. *Brain Res* **2018**, *1693*, 128-133.
2. Qi, X.; Yun, C.; Pang, Y.; Qiao, J. The impact of the gut microbiota on the reproductive and metabolic endocrine system. *Gut Microbes* **2021**, *13*, 1-21.
3. Xu, H.; Wang, X.; Feng, W.; Liu, Q.; Zhou, S.; Liu, Q.; Cai, L. The gut microbiota and its interactions with cardiovascular disease. *Microb Biotechnol* **2020**, *13*, 637-656.
4. Jiang, C.; Li, G.; Huang, P.; Liu, Z.; Zhao, B. The Gut Microbiota and Alzheimer's Disease. *J Alzheimers Dis* **2017**, *58*, 1-15.
5. CHOJI KANEUCHI, T.M. Bacteroides microfusus, a New Species from the Intestines of Calves, Chickens, and Japanese Quails. *International Journal of Systematic and Evolutionary Microbiology* **1978**, *28*, 478-481.
6. Gargari, G.; Taverniti, V.; Balzaretti, S.; Ferrario, C.; Gardana, C.; Simonetti, P.; Guglielmetti, S. Consumption of a Bifidobacterium bifidum Strain for 4 Weeks Modulates Dominant Intestinal Bacterial Taxa and Fecal Butyrate in Healthy Adults. *Appl Environ Microbiol* **2016**, *82*, 5850-5859.
7. Lopetuso, L.R.; Petito, V.; Graziani, C.; Schiavoni, E.; Paroni Sterbini, F.; Poscia, A.; Gaetani, E.; Franceschi, F.; Cammarota, G.; Sanguinetti, M.; et al. Gut Microbiota in Health, Diverticular Disease, Irritable Bowel Syndrome, and Inflammatory Bowel Diseases: Time for Microbial Marker of Gastrointestinal Disorders. *Dig Dis* **2018**, *36*, 56-65.
8. Morgan, X.C.; Tickle, T.L.; Sokol, H.; Gevers, D.; Devaney, K.L.; Ward, D.V.; Reyes, J.A.; Shah, S.A.; LeLeiko, N.; Snapper, S.B.; et al. Dysfunction of the intestinal microbiome in inflammatory bowel disease and treatment. *Genome Biol* **2012**, *13*, R79.
9. Liu, X.; Zeng, B.; Zhang, J.; Li, W.; Mou, F.; Wang, H.; Zou, Q.; Zhong, B.; Wu, L.; Wei, H.; et al. Role of the Gut Microbiome in Modulating Arthritis Progression in Mice. *Sci Rep* **2016**, *6*, 30594.
10. Cox, L.M.; Yamanishi, S.; Sohn, J.; Alekseyenko, A.V.; Leung, J.M.; Cho, I.; Kim, S.G.; Li, H.; Gao, Z.; Mahana, D.; et al. Altering the intestinal microbiota during a critical developmental window has lasting metabolic consequences. *Cell* **2014**, *158*, 705-721.
11. Liao, Y.; Peng, Z.; Chen, L.; Nüssler, A.K.; Liu, L.; Yang, W. Deoxynivalenol, gut microbiota and immunotoxicity: A potential approach? *Food Chem Toxicol* **2018**, *112*, 342-354.
12. Cani, P.D.; Possemiers, S.; Van de Wiele, T.; Guiot, Y.; Everard, A.; Rottier, O.; Geurts, L.; Naslain, D.; Neyrinck, A.; Lambert, D.M.; et al. Changes in gut microbiota control inflammation in obese mice through a mechanism involving GLP-2-driven improvement of gut permeability. *Gut* **2009**, *58*, 1091-1103.
13. Zhang, X.; Zhao, Y.; Zhang, M.; Pang, X.; Xu, J.; Kang, C.; Li, M.; Zhang, C.; Zhang, Z.; Zhang, Y.; et al. Structural changes of gut microbiota during berberine-mediated prevention of obesity and insulin resistance in high-fat diet-fed rats. *PLoS One* **2012**, *7*, e42529.
14. Xu, B.; Yan, Y.; Huang, J.; Yin, B.; Pan, Y.; Ma, L. Cortex Phellodendri extract's anti-diarrhea effect in mice related to its modification of gut microbiota. *Biomed Pharmacother* **2020**, *123*, 109720.
15. Liu, S.; Yang, B.; Yang, P.; Liu, Z. Herbal Formula-3 ameliorates OVA-induced food allergy in mice may via modulating the gut microbiota. *Am J Transl Res* **2019**, *11*, 5812-5823.
16. Palmas, V.; Pisanu, S.; Madau, V.; Casula, E.; Deledda, A.; Cusano, R.; Uva, P.; Vascellari, S.; Loviselli, A.; Manzin, A.; et al. Gut microbiota markers associated with obesity and overweight in Italian adults. *Sci Rep* **2021**, *11*, 5532.
17. Ebrahimzadeh Leylabadlo, H.; Sanaie, S.; Sadeghpour Heravi, F.; Ahmadian, Z.; Ghotaslou, R. From role of gut microbiota to microbial-based therapies in type 2-diabetes. *Infect Genet Evol* **2020**, *81*, 104268.
18. Ojo, O.; Feng, Q.Q.; Ojo, O.O.; Wang, X.H. The Role of Dietary Fibre in Modulating Gut Microbiota Dysbiosis in Patients with Type 2 Diabetes: A Systematic Review and Meta-Analysis of Randomised Controlled Trials. *Nutrients* **2020**, *12*.
19. Wu, C.; Fei, J.; Xu, Q.; Tao, Y.; Zhou, Z.; Wang, Y.; Wu, J.; Gu, H.F. Interaction between Plasma Metabolomics and Intestinal Microbiome in db/db Mouse, an Animal Model for Study of Type 2 Diabetes and Diabetic Kidney Disease. *Metabolites* **2022**, *12*.
20. Andersen, K.; Kesper, M.S.; Marschner, J.A.; Konrad, L.; Ryu, M.; Kumar Vr, S.; Kulkarni, O.P.; Mulay, S.R.; Romoli, S.; Demleitner, J.; et al. Intestinal Dysbiosis, Barrier Dysfunction, and Bacterial Translocation Account for CKD-Related Systemic Inflammation. *J Am Soc Nephrol* **2017**, *28*, 76-83.
21. Yang, T.; Richards, E.M.; Pepine, C.J.; Raizada, M.K. The gut microbiota and the brain-gut-kidney axis in hypertension and chronic kidney disease. *Nat Rev Nephrol* **2018**, *14*, 442-456.
22. Cai, T.T.; Ye, X.L.; Li, R.R.; Chen, H.; Wang, Y.Y.; Yong, H.J.; Pan, M.L.; Lu, W.; Tang, Y.; Miao, H.; et al. Resveratrol Modulates the Gut Microbiota and Inflammation to Protect Against Diabetic Nephropathy in Mice. *Front Pharmacol* **2020**, *11*, 1249.
23. Jiang, H.; Ling, Z.; Zhang, Y.; Mao, H.; Ma, Z.; Yin, Y.; Wang, W.; Tang, W.; Tan, Z.; Shi, J.; et al. Altered fecal microbiota composition in patients with major depressive disorder. *Brain Behav Immun* **2015**, *48*, 186-194.

24. Sun, Y.; Pei, J.; Chen, X.; Lin, M.; Pan, Y.; Zhang, Y.; Bai, W.; Zhou, X.; Zhang, W. The role of the gut microbiota in depressive-like behavior induced by chlorpyrifos in mice. *Ecotoxicol Environ Saf* **2023**, *250*, 114470.

25. Kutsyr, O.; Maestre-Carballa, L.; Lluesma-Gomez, M.; Martinez-Garcia, M.; Cuenca, N.; Lax, P. Retinitis pigmentosa is associated with shifts in the gut microbiome. *Sci Rep* **2021**, *11*, 6692.

26. Rowan, S.; Taylor, A. The Role of Microbiota in Retinal Disease. *Adv Exp Med Biol* **2018**, *1074*, 429-435.

27. Dinh, D.M.; Volpe, G.E.; Duffalo, C.; Bhalchandra, S.; Tai, A.K.; Kane, A.V.; Wanke, C.A.; Ward, H.D. Intestinal microbiota, microbial translocation, and systemic inflammation in chronic HIV infection. *J Infect Dis* **2015**, *211*, 19-27.

28. Lozupone, C.A.; Li, M.; Campbell, T.B.; Flores, S.C.; Linderman, D.; Gebert, M.J.; Knight, R.; Fontenot, A.P.; Palmer, B.E. Alterations in the gut microbiota associated with HIV-1 infection. *Cell Host Microbe* **2013**, *14*, 329-339.

29. Mutlu, E.A.; Keshavarzian, A.; Losurdo, J.; Swanson, G.; Siewe, B.; Forsyth, C.; French, A.; Demarais, P.; Sun, Y.; Koenig, L.; et al. A compositional look at the human gastrointestinal microbiome and immune activation parameters in HIV infected subjects. *PLoS Pathog* **2014**, *10*, e1003829.

30. Vujkovic-Cvijin, I.; Dunham, R.M.; Iwai, S.; Maher, M.C.; Albright, R.G.; Broadhurst, M.J.; Hernandez, R.D.; Lederman, M.M.; Huang, Y.; Somsouk, M.; et al. Dysbiosis of the gut microbiota is associated with HIV disease progression and tryptophan catabolism. *Sci Transl Med* **2013**, *5*, 193ra191.

31. Bai, B.; Wang, X.; Li, Y.; Chen, P.C.; Yu, K.; Dey, K.K.; Yarbro, J.M.; Han, X.; Lutz, B.M.; Rao, S.; et al. Deep Multilayer Brain Proteomics Identifies Molecular Networks in Alzheimer's Disease Progression. *Neuron* **2020**, *105*, 975-991.e977.

32. Chen, Q.; Wu, J.; Dong, X.; Yin, H.; Shi, X.; Su, S.; Che, B.; Li, Y.; Yang, J. Gut flora-targeted photobiomodulation therapy improves senile dementia in an Aß-induced Alzheimer's disease animal model. *J Photochem Photobiol B* **2021**, *216*, 112152.

33. Feng, M.; Hou, T.; Zhou, M.; Cen, Q.; Yi, T.; Bai, J.; Zeng, Y.; Liu, Q.; Zhang, C.; Zhang, Y. Gut microbiota may be involved in Alzheimer's disease pathology by dysregulating pyrimidine metabolism in APP/PS1 mice. *Front Aging Neurosci* **2022**, *14*, 967747.

34. Nimjee, S.M.; White, R.R.; Becker, R.C.; Sullenger, B.A. Aptamers as Therapeutics. *Annu Rev Pharmacol Toxicol* **2017**, *57*, 61-79.

35. Ellington, A.D.; Szostak, J.W. In vitro selection of RNA molecules that bind specific ligands. *Nature* **1990**, *346*, 818-822.

36. Gan, Z.; Roslan, M.A.M.; Abd Shukor, M.Y.; Halim, M.; Yasid, N.A.; Abdullah, J.; Md Yasin, I.S.; Wasoh, H. Advances in Aptamer-Based Biosensors and Cell-Internalizing SELEX Technology for Diagnostic and Therapeutic Application. *Biosensors (Basel)* **2022**, *12*.

37. Tuerk, C.; Gold, L. Systematic evolution of ligands by exponential enrichment: RNA ligands to bacteriophage T4 DNA polymerase. *Science* **1990**, *249*, 505-510.

38. Cho, G.; Keefe, A.D.; Liu, R.; Wilson, D.S.; Szostak, J.W. Constructing high complexity synthetic libraries of long ORFs using in vitro selection. *J Mol Biol* **2000**, *297*, 309-319.

39. Komarova, N.; Kuznetsov, A. Inside the Black Box: What Makes SELEX Better? *Molecules* **2019**, *24*.

40. Kubiczek, D.; Raber, H.; Bodenberger, N.; Oswald, T.; Sahan, M.; Mayer, D.; Wiese, S.; Stenger, S.; Weil, T.; Rosenau, F. The Diversity of a Polyclonal FluCell-SELEX Library Outperforms Individual Aptamers as Emerging Diagnostic Tools for the Identification of Carbapenem Resistant Pseudomonas aeruginosa. *Chemistry* **2020**, *26*, 14536-14545.

41. Raber, H.F.; Kubiczek, D.H.; Bodenberger, N.; Kissmann, A.K.; D'Souza, D.; Xing, H.; Mayer, D.; Xu, P.; Knippschild, U.; Spellerberg, B.; et al. FluCell-SELEX Aptamers as Specific Binding Molecules for Diagnostics of the Health Relevant Gut Bacterium Akkermansia muciniphila. *Int J Mol Sci* **2021**, *22*.

42. Xing, H.; Kissmann, A.K.; Raber, H.F.; Krämer, M.; Amann, V.; Kohn, K.; Weil, T.; Rosenau, F. Polyclonal Aptamers for Specific Fluorescence Labeling and Quantification of the Health Relevant Human Gut Bacterium Parabacteroides distasonis. *Microorganisms* **2021**, *9*.

43. Xing, H.; Zhang, Y.; Krämer, M.; Kissmann, A.K.; Amann, V.; Raber, H.F.; Weil, T.; Stieger, K.R.; Knippschild, U.; Henkel, M.; et al. A Polyclonal Aptamer Library for the Specific Binding of the Gut Bacterium Roseburia intestinalis in Mixtures with Other Gut Microbiome Bacteria and Human Stool Samples. *Int J Mol Sci* **2022**, *23*.

44. Xing, H.; Zhang, Y.; Krämer, M.; Kissmann, A.K.; Henkel, M.; Weil, T.; Knippschild, U.; Rosenau, F. A Polyclonal Selex Aptamer Library Directly Allows Specific Labelling of the Human Gut Bacterium Blautia producta without Isolating Individual Aptamers. *Molecules* **2022**, *27*.

45. Zhou, J.; Rossi, J.J. Evolution of Cell-Type-Specific RNA Aptamers Via Live Cell-Based SELEX. *Methods Mol Biol* **2016**, *1421*, 191-214.

46. Koh, A.Y. Potential for Monitoring Gut Microbiota for Diagnosing Infections and Graft-versus-Host Disease in Cancer and Stem Cell Transplant Patients. *Clin Chem* **2017**, *63*, 1685-1694.

47. Bhalla, N.; Jolly, P.; Formisano, N.; Estrela, P. Introduction to biosensors. *Essays Biochem* **2016**, *60*, 1-8.

13

48. Ni, S.; Zhuo, Z.; Pan, Y.; Yu, Y.; Li, F.; Liu, J.; Wang, L.; Wu, X.; Li, D.; Wan, Y.; et al. Recent Progress in Aptamer Discoveries and Modifications for Therapeutic Applications. *ACS Appl Mater Interfaces* **2021**, *13*, 9500-9519.

49. Rasoulinejad, S.; Gargari, S.L.M. Aptamer-nanobody based ELASA for specific detection of Acinetobacter baumannii isolates. *J Biotechnol* **2016**, *231*, 46-54.

50. Dua, P.; Kim, S.; Lee, D.K. Nucleic acid aptamers targeting cell-surface proteins. *Methods* **2011**, *54*, 215-225.

51. Walker, A.W.; Duncan, S.H.; Louis, P.; Flint, H.J. Phylogeny, culturing, and metagenomics of the human gut microbiota. *Trends Microbiol* **2014**, *22*, 267-274.

52. Kissmann, A.K.; Andersson, J.; Bozdogan, A.; Amann, V.; Krämer, M.; Xing, H.; Raber, H.F.; Kubiczek, D.H.; Aspermair, P.; Knoll, W.; et al. Polyclonal aptamer libraries as binding entities on a graphene FET based biosensor for the discrimination of apo- and holo-retinol binding protein 4. *Nanoscale Horiz* **2022**, *7*, 770-778.

53. Lilja, S.; Stoll, C.; Krammer, U.; Hippe, B.; Duszka, K.; Debebe, T.; Höfinger, I.; König, J.; Pointner, A.; Haslberger, A. Five Days Periodic Fasting Elevates Levels of Longevity Related Christensenella and Sirtuin Expression in Humans. *Int J Mol Sci* **2021**, *22*.